Carbon corrosion of alloys at high temperature

by D.J. Young* and J. Zhang*

Synopsis

Alloys used at high temperature must resist both creep and corrosion. Design for corrosion resistance is based on the formation of a slow-growing, protective oxide scale by selective oxidation of an appropriate alloy component, usually chromium or aluminium. A successful scale will exclude other corrodents, notably carbon, which can otherwise cause extremely rapid corrosion at high temperatures.

Selective oxidation of an alloy component necessarily lowers the concentration of that metal in the alloy subsurface region. Under thermal cycling conditions, mechanical damage to the scale leads to renewed oxide growth and accelerated alloy depletion. Eventually, a point is reached where diffusion of a corrodent into the alloy becomes competitive with the outward diffusion of alloy metal to repair the protective scale. Two examples of alloy failure by carbon attack are considered.

In the steam cracking (pyrolysis) process, centrifugally cast tubes of heat-resisting alloy are exposed to a gas stream of hydrocarbon and steam, at a carbon activity of unity. Formation and repair of the surface chromia scale causes alloy depletion, Kirkendall void formation, and subsequent internal precipitation of chromium-rich carbides. Their formation makes chromia scale formation much more difficult, and generates internal stress. Eventually, the tubes fail by creep rupture.

In other processes (e.g. steam reforming, heat treatment), synthesis gases are supersaturated with carbon at intermediate temperatures. Once the alloy's protective scale is breached, carbon attacks the depleted substrate. In the case of ferritic alloys, it forms a surface scale of Fe_3C. As this scale thickens, the supersaturated carbon precipitates as graphite within its outer regions. The resulting volume expansion causes disintegration of the cementite in a process known as metal dusting.

In the case of austenitic alloys, no metal carbide is formed. Instead, carbon dissolves in the depleted metal to diffuse inward and precipitate as graphite within the metal matrix. Again, volume expansion causes disintegration of the alloy, and metal dusting results. Dusting occurs at an extraordinarily rapid rate, and leads to failure by section loss or even penetration.

Keywords
high-temperature corrosion, oxidation, carburization, metal dusting.

Introduction

Carbon is unique among the common oxidants in being stable as a solid if the environment is sufficiently reducing. For this reason, the thermodynamic reference state is chosen as pure, solid graphite, for which $a_C = 1$. If the carbon activity is less than unity, but large enough to stabilize a metal carbide, the reaction is described as carburization. In such processes, internally precipitated carbides develop rapidly and alloy destruction can result. Because carbides are much less stable than the corresponding oxides, carburization is a problem only under reducing conditions. The necessary conditions arise in particular gases encountered in e.g. petrochemical processes such as steam cracking (pyrolysis). They can also develop at an alloy-scale interface, where the oxygen potential is maintained at a low value by the local equilibrium

$$M + \tfrac{1}{2}O_2(g) = MO \qquad [1]$$

This situation is a problem only if carbon can penetrate the oxide scale.

If the gas is supersaturated with respect to carbon ($a_C > 1$), an even greater threat emerges. If the gas can be equilibrated, carbon is released from the gas phase and deposits in a process described as coking. Often, however, gases remain supersaturated. In this event, catalysis of carbon deposition by the metal can lead to its disruption and fragmentation in an extremely rapid corrosion process known as metal dusting.

Carbon activities

Gas phase processes producing carbon include the synthesis gas reaction

$$CO + H_2 = H_2O + C \qquad [2]$$

the Boudouard reaction

$$2CO = CO_2 + C \qquad [3]$$

and hydrocarbon cracking, e.g.

* *University of New South Wales, Sydney.*

ISSN 2225-6253. This paper was first presented at the, Ferrous and Base Metals Development Network Conference 2012, 15–17 October 2012, Mount Grace Country House and Spa, Magaliesburg, South Africa..

$$CH_4 = 2H_2 + C \quad [4]$$

The standard free energies of these reactions are listed in Table I. All three reactions are very slow as homogenous gas phase processes, and they will not reach equilibrium in a typical laboratory reactor, unless catalysed. Although many materials of practical interest, such as iron, nickel, cobalt, and their alloys, are catalytically active to these reactions, their oxide scales are inert.

As seen in Table I, temperature effects are very different for these carbon-producing reactions. Thus methane and hydrocarbons in general can produce significant carbon activities only at high temperatures. On the other hand, the synthesis gas and Boudouard reactions result in increasing carbon activities as temperatures are lowered.

Carburization reactions in steam cracking conditions

Pyrolysis or 'steam cracking' tubular reactors are used for making ethylene or propylene, e.g.

$$(H_2O) + C_2H_6 = C_2H_4 + H_2 + (H_2O) \quad [5]$$

Hydrocarbon cracking also produces carbon, and $a_c \approx 1$. Steam acts as a diluent in order to reduce the amount of solid carbon produced by gas phase pyrolysis, and also provides an oxidant to passivate tube metal surfaces. Rising prices of feedstock hydrocarbons and the need for improved process efficiencies have led to higher operating temperatures. Simultaneously, tube wall thicknesses have been reduced to improve heat transfer efficiency. Thus process engineering changes have led to higher tube metal temperatures and reduced load-bearing sections. These increased demands on material properties have been met by a series of advances in alloy design. The tubes are centrifugally cast, austenitic chromia-formers. Their compositions (Table II) have evolved from the old HK 40 grade (Fe-25Cr-20Ni), through the HP grades (Fe-25Cr-35Ni) to high-nickel alloys containing 45% or even 60% Ni. The increased alloy levels have provided significant improvements in creep properties, but the alloys are still subject to corrosion by carbon.

The general appearance of cast heat-resistant alloys after exposure to simulated reaction conditions is shown in Figure 1. Both alloys shown have developed chromium-rich oxide scales, causing chromium depletion from the underlying alloy and dissolution of chromium-bearing carbides from the subsurface zone. Major differences are apparent deeper within the alloys: in Figure 1(a) no damage has occurred, apart from coarsening of the original interdendritic carbides, whereas in Figure 1(b) massive internal carburization is obvious. The latter effect leads to swelling of the metal. If allowed to continue, this process eventually leads to creep rupture.

The different behaviour of the two alloys is due to their different chemistries and the resulting subsurface oxidation. Minority components silicon and aluminium lead to development of a continuous oxide layer beneath the chromia scale in one case (Figure. 1(a)). This slows the chromia scale growth rate and simultaneously improves its ability to block carbon entry. The alloy shown in Figure 1(b) has a low silicon content (0.6 wt%), insufficient to form a continuous layer, and internal precipitation of SiO_2 results. As a result, the chromia scale grows more rapidly, leading to Kirkendall voids developing in the subsurface alloy region. In the absence of a continuous silica (or alumina) sublayer, the chromia scale is unable to block carbon entry, and internal carbide precipitation results.

Many laboratory studies of carburization have led to a good understanding of the process[1]. It is commonly observed[2–4] that exposure of heat-resisting alloys to gas compositions such that no chromia scale can form leads to internal chromium carbide precipitation rather than external scale formation. Carbon dissolves in the alloy and diffuses inwards to react with chromium and precipitate chromium carbides. Carbon diffusion controls the rate at which the carbide precipitation zone depth, X_i, increases with time, t, and parabolic kinetics result:

$$X_i^2 = 2k_p^{(i)}t \quad [6]$$

According to Wagner's theory[5], when the carbon permeability in the alloy is high

$$k_p^{(i)} = \frac{\varepsilon N_c^{(s)} D_c}{\nu N_M^{(o)}} \quad [7]$$

where $N_C^{(s)}$ is the concentration of dissolved carbon at the alloy surface, D_C the carbon diffusion coefficient in the

Table I

Standard free energies of reactions

Reaction	$\Delta G^\circ = A + BT$ (Jmol^{-1})	
	A	*B*
$CO + H_2 = H_2O + C$	-134 515	142.37
$2CO = CO2 + C$	-170 700	174.5
$CH_4 = 2H_2 + C$	87 399	-108.74

Table II

Some nominal heat-resisting alloy compositions (wt%)

Alloy	C	Si	Mn	Ni	Cr	Nb	Al	Other
HK40	0.4	1.3	0.6	21	25			
HP	0.4	1.8	1.1	35	25	0.8		0.1Zr,0.2Ti
HP Mod Nb	0.44	1.5	1.5	35	25	1.5		
H101	0.09	2.2	1.1	36	26	1		
30Cr Micro	0.53	2.1	0.3	29	30	1		0.11Ce
35/45	0.46	2.1	1.2	45	35	1		
45Pa	0.45	1	0.4	45	19	0.4	2	3Mo,0.3-1.5Hf
45HT	0.44	1	0.5	45	30	0.5	0.5	0-0.8Hf

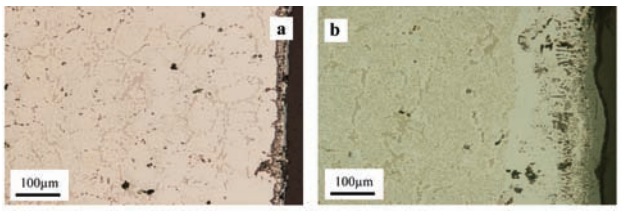

Figure 1—General appearance of cast heat-resisting alloys after 500 h exposure to steam-hydrocarbon mixture at 1100°C: (a) high-silicon, aluminium-bearing version, and (b) low-silicon version of HP grade

chromium-depleted alloy matrix, $N_M^{(o)}$ the original alloy concentration of metal M which forms carbide MC_v, and ε a factor accounting for diffusional blocking by precipitates. Thus carburization rates are predicted to vary inversely with the concentration of reactive solute metal.

Carburization of Fe-Cr alloys[6,7] produces chromium-rich $(Cr,Fe)_7C_3$ precipitates, and follows parabolic kinetics. Plots of $k_P^{(i)}$ against $1/N_{Cr}^{(o)}$ were shown to be linear except at high $N_{Cr}^{(o)}$ values. The slopes of these lines were used together with $v = 0.71$ (for $(Cr_{0.6}Fe_{0.4})_7C_3$ formed by low-chromium alloys) and the assumption $\varepsilon = 1$ to calculate carbon permeabilities. Comparison in Table III with values found from independently measured $N_c^{(s)}$ and D_c values[8,9] shows good agreement, demonstrating the utility of Equation [7] in describing carburization rates.

Equation [7] is based on the assumption of very stable carbide precipitates and the complete removal of chromium from the alloy by carburization. In fact, this is a poor approximation, and significant levels of chromium remain in the alloy matrix[1]. This has the effect of decreasing the effective value of $N_{Cr}^{(o)}$ appearing in Equation [7], leading to the prediction of an enhanced value of $k_p^{(i)}$. However, the effect is not large, and uncertainties in measured values of $N_c^{(s)}$, D_c, and $k_p^{(i)}$ total at least the same amount of error. It is concluded that Wagner's simple result (Equation [7]) allows good order–of-magnitude prediction for model alloy carburization. More importantly, it also provides good predictions for commercial alloy carburization rates, as seen in Table IV.

Alloy composition affects carburization rates in a number of ways. Carbon permeability, $N_C^{(s)}D_C$, varies strongly with alloy Fe/Ni ratio, as shown in Figure 2. A minimum is found for nickel-base alloys of Inconel-type compositions, this value being about 1/5–1/3 times that of a standard HP grade.

Minority alloy components are also important. Carbide-formers such as molybdenum participate in precipitation reactions. The effect on kinetics can be predicted[10] by adjusting the effective value of $N_M^{(o)}$ in Equation [7] to account for the additional precipitating metal. Other carbide-formers such as niobium and reactive elements are often present, although at low levels. They have unexpectedly large effects in reducing carburization rates, for reasons which are unclear[1]. Silicon slows carburization[11], even when the gas is not oxidizing to the solute metal. The effect results from the depression of carbon solubility by silicon, and its negative effect on D_C.

While alloy compositional effects on carburization are reasonably well understood, it remains the case that acceptable carburization resistance cannot be achieved in the absence of an external oxide scale.

Metal dusting in synthesis gas

Synthesis gas can be produced in the steam reforming reaction

$$CH_4 + H_2O = CO + 3H_2 \quad [8]$$

at the operating temperatures of 800–900°C, where $a_c < 0.5$. However, as the product gas cools below about 700°C, the equilibrium constant K_2 increases, a_c becomes supersaturated, and the possibility of metal dusting arises. Metal dusting is a catastrophic form of corrosion in which metals exposed to carbon-supersaturated gas disintegrate, forming metal-rich particles (the 'dust') dispersed in a voluminous carbon deposit. Rates of alloy consumption can be

Table III

Carbon permeabilities $N_C^{(s)}D_C$ (cm^2s^{-1}) in Fe-Cr

	900°C	1 000°C	1 100°C
From Equation [7]	6.6×10^{-9}	2.5×10^{-8}	6.2×10^{-8}
From $N_C^{(s)}$ and D_c	4.3×10^{-9}	1.4×10^{-8}	5.5×10^{-8}

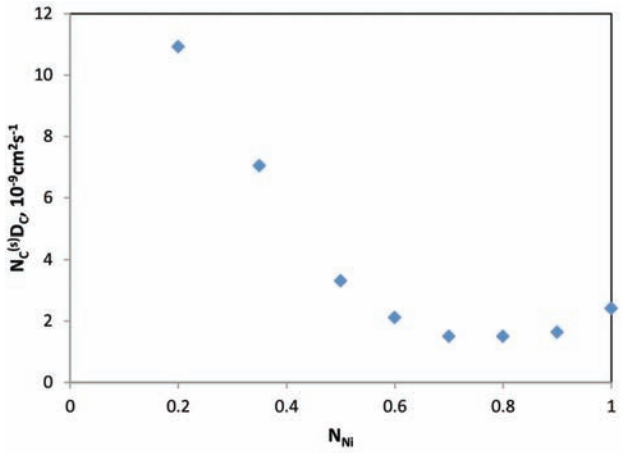

Figure 2—Carbon permeability as a function of alloy composition for Fe-Ni alloys at 1000°C with unit carbon activity

Table IV

Carburization rate constants 10^7k_P (cm^2s^{-1})

	900°C		1 000°C	1 100°C		
	Measured	Calculated	Measured	Calculated	Measured	Calculated
G4868	0.10	0.11	0.13	0.33	1.45	2.05
G4852	0.18	0.10	0.28	0.37	0.64	2.15
H101	0.06	0.06	0.17	0.24	0.44	1.32
Fe-35Cr-45Ni	0.04	0.03	0.10	0.08	0.44	0.50
45Pa	0.05-0.08	0.034	0.13-0.22	0.18	0.41-0.43	0.99
45HT	0.04-0.05	0.023	0.10-0.15	0.15	0.63	0.62

remarkably fast, leading to potentially dangerous conditions. Although heat-resisting alloys are initially able to withstand this attack, the subsequent onset of the dusting process is difficult to predict, and its development can go undetected.

Early reports of industrial failures[12–15] were followed by the research of Hochman[16–18] on dusting of iron, nickel, cobalt, and chromia-forming ferritic and austenitic alloys. Subsequent work by Grabke[19–23] quantified and extended Hochman's observations. More recent work by the authors[24–35] and others[36–41] has clarified some of the more mysterious aspects of dusting process.

Iron, nickel, cobalt, and their alloys are catalytic to the reactions in Equations [2]–[4], and carbon deposition results from contact of these gases with common structural metals. Understanding how catalysis of carbon release from a gas disrupts and fragments the catalytic metal requires a detailed consideration of reaction morphologies and mechanisms.

Practical alloys form protective oxide scales, usually chromia, which can act as a barrier to carbon ingress. However, at the relatively low temperatures involved, alloy diffusion is rather slow, and the ability of these alloys to reheal damaged scales is limited. Once this capacity is exhausted, carbon attacks the chromium-depleted substrate. The mechanism and morphology of this reaction is in most respects characteristic of the dusting of alloy basis metals: iron, nickel, or Fe-Ni. Different mechanisms apply to ferritic and austenitic alloys.

Dusting of iron

Iron and low-alloy steels exposed to carbon-supersaturated gas grow external scales of cementite, Fe_3C. In the early stages of reaction, the scale thickness, X, grows according to parabolic kinetics:

$$X^2 = 2k_p t \qquad [9]$$

and the rate is controlled by inward diffusion of C through the scale[42]. At the same time, the mass of coke deposited on top of the scale and the quantity of iron consumed both increase. The coke deposit is highly porous, consisting largely of graphite nanotubes and filaments which are decorated with cementite nanoparticles[24–26,31,33]. Thus iron is consumed in producing the cementite scale and the large numbers of Fe_3C particles (the 'dust').

The cementite dust forms by disintegration of the scale outer surface. At longer reaction times, the overall change in scale thickness with reaction time represents the net outcome of the growth and disintegration processes:

$$\frac{dX}{dt} = \frac{k_p}{X} - k_d \qquad [10]$$

where k_d is the linear rate constant for cementite scale loss. The disintegration is attributed to nucleation of graphite at favourable sites within the cementite, and the resulting volume expansion. Graphite precipitation is possible because carbon activities are necessarily greater than unity within the Fe_3C, in order for that phase to exist. Growth of the graphite is supported by continuing diffusion of carbon through the Fe_3C lattice. The source of the carbon is catalysis at the scale surface of reactions such as Equations [2] and [3].

Continued growth of coke filaments occurs via the same mechanism. Exposed facets of Fe_3C nanoparticles catalyse release of carbon from the gas phase. This carbon diffuses through the particle toward other facets which are energetically favourable for graphite deposition. At these positions, the carbon attaches to the graphite filament, lengthening it and displacing the cementite particle outward. The overall process is shown schematically in Figure 3. Because the resulting coke structure is highly porous, the gas is able to penetrate it, reaching the cementite scale surface where further catalysis of carbon release is therefore possible.

Dusting of nickel

Metal dusting of nickel and austenitic alloys differs from the reaction of ferritic materials in that cementite is not formed, and the corresponding nickel carbide is unstable. An examination of the dusting behaviour of pure nickel provides a good basis for understanding the reaction of austenitic heat-resisting alloys.

Dusting of nickel is much slower than the corresponding reaction for iron. It produces the reaction morphology shown in Figure 4, where the carbon deposit is in direct contact with the metal, and is growing into it[28,30,39,40]. The metal-graphite interface is seen in Figure 4 to be faceted, and reflects the preferred orientation relationship $(0001)_{Gr}//(111)_{Ni}$. It is the development of this energetically favoured interface at an angle to the metal surface which allows graphite nucleation within the carbon-supersaturated metal. Growth of the graphite nuclei causes volume expansion and disruption of the metal.

Its disintegration produces the nickel nanoparticles seen in Figure 4. When exposed to gas, these particles catalyse the release of more carbon and its deposition at crystallographically favoured sites to grow the nanofilaments, as shown in Figure 4.

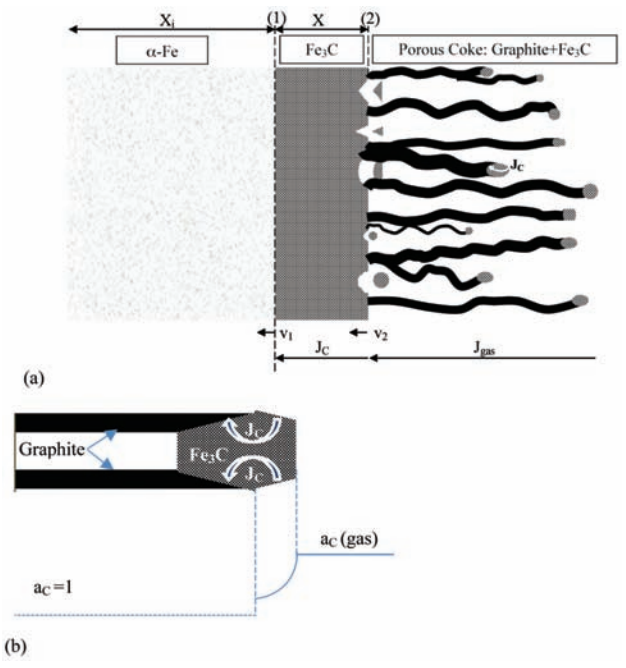

Figure 3—Schematical diagram showing (a) the process of iron dusting and (b) carbon diffusion through Fe_3C particles for continuous graphite nanotube formation

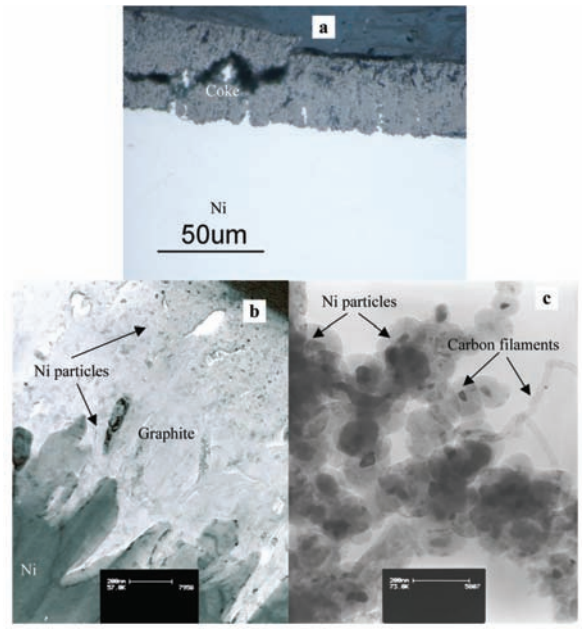

Figure 4—(a) and (b): metallographic and TEM cross-sections, respectively, and (c) TEM surface coke morphologies of pure nickel after metal dusting

The continued growth of graphite into the metal requires a supply of carbon, which is available only by diffusion through the substrate nickel. This is possible because the nickel surface remains in contact with a high carbon activity, which is available from the gas. The dusting reaction product is a two-phase mixture of graphite plus nickel which is gas permeable, and at uniform carbon and nickel activities throughout its thickness. Carbon is transported through the coke via the gas phase. Nickel transport is not via diffusion; instead, nickel particles are displaced outwards by accumulating graphite.

The requirement for dusting, that graphite basal planes be oriented at an angle to the surface, is not related to nickel surface orientation, and cannot thereby be controlled. Prevention of dusting requires either a surface barrier to carbon entry or disruption of the $\{0001\}_{Gr}//\{111\}_{Ni}$ relationship by alloying[27,29,34,35].

Graphite nucleation is made more difficult by alloying with Cu, which forms no carbide and is non-catalytic to coke. Adding copper to Ni[27], austenitic Fe-Ni[35] and austenitic stainless steels[29] markedly decreases carbon uptake.

Protection against carbon corrosion

Surface oxide scales play a critical role in the long-term behaviour of practical alloys exposed to carbon-rich gases. Isotope experiments have shown[43] that the solubility of carbon in Cr_2O_3 and Al_2O_3 at 1000°C is extremely low. Scales of these oxides are therefore expected to provide effective diffusion barriers to carbon. Furthermore, most observations suggest that these oxides provide no significant catalysis of carbon deposition from the gas[44]. To remain effective, such a scale must retain its mechanical integrity and chemical stability.

In the atmospheres of interest, Cr_2O_3, Al_2O_3, SiO_2, and $FeCr_2O_4$ are all stable (and stable with respect to the corresponding carbides), and the usual heat-resisting alloy designs are on this basis expected to succeed. However, many alloys nonetheless fail by carburization or dusting. In the case of dusting, an important factor is the rather modest temperature involved, and the consequently slow alloy diffusion. For example, a standard material such as Alloy 800 (about 20 wt% Cr) dusts rapidly at temperatures of 60–700°C[45,46].

The onset of heat-resisting alloy dusting has been observed by Grabke and co-workers[20,22,47] under isothermal conditions, and by Toh *et al.*[24,45,48] under temperature cycling conditions. Selective oxidation of chromium produces a Cr_2O_3 scale and a chromium-depleted subsurface alloy region, until local scale damage allows gas access to the metal. If sufficient chromium remains, the Cr_2O_3 scale reheals; if not, other reactions follow. Commonly, p_{O_2} is too low for nickel or iron oxides to form and, instead, carbon enters the alloy, precipitating chromium carbides. Immobilization of chromium in this way renders future oxide healing of the surface impossible, and gas access to the chromium-depleted surface continues. The surface is now essentially an Fe-Ni alloy. At high nickel levels it undergoes graphitization and disintegration in the same way as pure nickel; ferritic alloys form cementite and dust in the same manner as iron.

Improved protection requires scales that resist spallation and cracking, and which remain impermeable to carbon. Superior protection against high-temperature carburization is achieved with alloys containing relatively high silicon levels (about 2%) plus small amounts of reactive elements. These alloys form a silica sublayer beneath their chromia scales, and maintain good scale adherence as a result of the reactive element effect. Even better resistance to carbon penetration is provided by alumina scales. Compositions that lead to alumina scale formation can be better suited to coatings than to structural alloys.

An alternative approach to resisting dusting attack (at temperatures where oxide scale formation can be difficult to maintain) is the use of copper alloying to inhibit graphite nucleation. New copper-bearing alloys have recently been developed for this purpose[44,49,50]. The dusting performance under cycling conditions of two such alloys is compared with that of Ni, Ni-20Cr, and the high-performance Haynes alloy 214 in Figure 5.

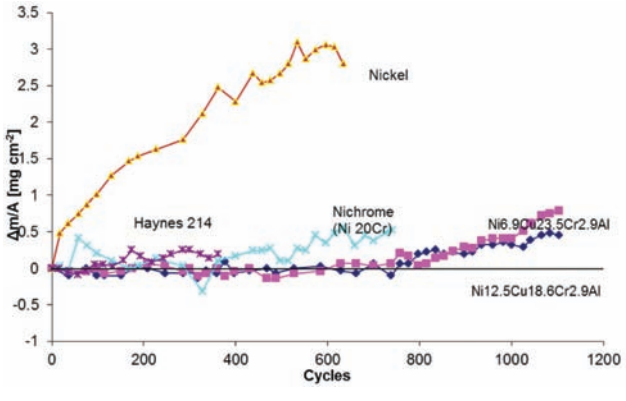

Figure 5—Carbon uptake during repeated 1 h cycles of exposure to a dusting gas at T = 650°C. Alloy compositions in wt% (after Speck and Young[50])

Carbon corrosion of alloys at high temperature

Summary and conclusions

Carburization reactions at $a_C \leq 1$ are successfully described by classical theory: solid-state diffusion of dissolved carbon controls the rate and parabolic kinetics result. Wagner's diffusion theory provides good quantitative prediction of rates, even for complex commercial alloys, providing that no oxide scale forms.

Metal dusting reactions at $a_C \geq 1$ involve complex mechanisms. Iron and ferritic alloys grow a cementite scale by inward carbon diffusion, a process that also leads to graphite nucleation within the cementite. Disintegration of the carbide produces particles which further catalyse the graphite deposition process, leading to the accumulation of large amounts of porous coke. Nickel and austenitic alloys do not form cementite, but catalyse the direct nucleation and growth of graphite. This occurs within the metal, disrupting its structure and producing a dust of austenite.

In all cases, the major mass transfer process is inward transport of carbon, either as a gas species through porous coke, or as a solute in catalytic material, either metal or cementite. The key to protection against both carburization and dusting is therefore blockage of inward carbon transport. In the case of lower temperature dusting reactions, the additional possibility of preventing the catalytic process of carbon release is available.

Catalysis can be prevented by altering the surface chemistry. Feasible methods of doing this are alloying austenitic materials with copper, coating with copper- or tin-rich materials, or poisoning with sulphur.

Carbon transport can be blocked by a scale of chromia or alumina. Achieving a chemically stable and mechanically resilient scale requires successful alloy design and sometimes high-temperature pre-oxidation. The alloy design needed to achieve the necessary oxide performance can require implementation as a coating rather than a structural alloy.

Acknowledgements

Support from the Australian Research Council and Schmidt & Clemens GmbH (Germany) is gratefully acknowledged.

References

1. Young, D.J. High Temperature Oxidation and Corrosion of Metals. First edition. Elsevier, 2008.
2. Grabke, H.J. Gravenhorst, U., and Steinkusch, W. Aufkohlung von chrom-nickel-eisen-stählen in der kohlenstoffpackung. *Werkstoffe und Korrosion*, vol. 27, 1976. pp. 291–296.
3. Schnaas, A. and Grabke, H.J. *Oxidation of Metals*, 12, 387 (1978).
4. Smith, G.M., Young, D.J., and Trimm, D.L. *Oxidation of Metals*, vol. 18, 1982. pp. 229.
5. Wagner, C. *Zeitschrift für Elektrochemie*, vol. 63, 1959. pp. 772.
6. Ahmed, O. and Young, D.J. Precipitate distributions in internally carburised and oxidised Fe-Cr alloys. *High Temperature Corrosion and Materials Chemistry II.* McNallan, M.J., Opila, E.J., Maruyama, T., and Narita, T. (eds). The Electrochemical Society, Inc., Pennington, NJ, 2000. pp. 77.
7. Young, D.J. and Ahmed, O. *Materials Science Forum*, vol. 369–372, 2001. pp. 93.
8. Wada, T., Wada, H., Elliott, J.F., and Chipman, J. *Metallurgical Transactons*, vol. 3, 1972. pp. 2865.
9. Smith, R.P. *Acta Metallurgica*, vol. 1, 1953. pp. 578-
10. Mitchell, D.R.G., Young, D.J., and Kleeman, W. *Materials and Corrosion*, vol. 49, 1998. pp. 231.
11. Kane, R.H. *Corrosion*, vol. 37, 1981. pp. 187.
12. Camp, E., Phillips, C., and Cross, L. *Corrosion*, vol. 10, 1954. pp. 149.
13. Hubbell, W.G. *The Iron Age*, vol. 157, 1946. pp. 56.
14. Burns, O.L. *Corrosion*, vol. 6, 1950. pp. 169.
15. Lefrancois, P.A. and Hoyt, W.B. *Corrosion*, vol. 19, 1963. pp. 360.
16. Hochman, R.F. Proceedings of the. *3rd International Congress of Metallic Corrosion*. University of Moscow Press, Moscow, 1969.
17. Hochman, R.F. and Klett, M.G. *Proceedings of the 5th International Congress of Metallic Corrosion*, NACE, Houston TX, 1974.
18. Hochman, R.F. Proceedings of the Symposium Properties of High Temperature Alloys with Emphasis on Environmental Effects. Foroulis, Z.A. and Pettit, E.S. (eds.). *E*lectrochemical Society, Pennington NJ, 1977. pp. 571.
19. Grabke, H.J., Hemptenmacher, J., and Munker, A. *Werkstoffe und Korrosion*, vol. 35, 1984. pp. 543.
20. Nava Paz, J.C. and Grabke, H.J. *Oxidation of. Metals*, vol. 39, 1993. pp. 437.
21. Grabke, H.J., Krajak, R., and Nava Paz, J.C. *Corrosion Science*, vol. 35, 1993. pp. 1141.
22. Grabke, H.J., Krajak, R., and Muller-Lorenz, E.M. *Werkstoffe und Korrosion*, vol. 44, 1993. pp. 89.
23. Grabke, H.J., Brancho-Trochonis, C.B., and Muller-Lorenz, E.M. *Werkstoffe und Korrosion*, vol. 56, 2007. pp. 281.
24. Toh, C.H., Munroe, P.R., and Young, D.J. *Oxidation of Metals*, vol. 58, 2002. pp. 1.
25. Zhang, J., Schneider, A., and Inden, G. *Corrosion Science*, vol. 45, 2003. pp. 281.
26. Zhang, J., Schneider, A., and Inden, G. *Corrosion Science*, vol. 45, 2003. pp. 1329.
27. Zhang, J., Cole, D.M.I., and Young, D.J. *Materials and Corrosion*, vol. 56, 2005. pp. 756.
28. Zhang, J. and Young, D.J. *Corrosion Science*, vol. 49, 2007. pp. 1496.
29. Zhang, J. and Young, D.J. *Corrosion Science*, vol. 49, 2007. pp. 1450.
30. Zhang, J., Munroe, P., and Young, D.J. *Acta Materialia*, vol. 56, 2008. pp. 68.
31. Zhang, J. and Young, D.J. *Oxidation Of Metals*, vol. 70, 2008. pp.
32. Zhang, J. and Young, D.J. *Corrososion Science*, vol. 51, 2009. pp. 2983.
33. Motin, M.A.A., Zhang, J., Munroe, P.R., and Young, D.J. *Corrosion Science*, vol. 52, 2010. pp. 3280.
34. Young, D.J., Zhang, J., Geers, C., and Schutz, M. *Materials and Corrosion*., vol. 62, 2011. pp. 7.
35. Zhang, J. and Young, D.J. *Corrosion Science*, vol. 56, 2012. pp. 184.
36. Pippel, E., Woltersdorf, J., and Schneider, R. *Materuals And Corrosion*, vol. 49, 1998. pp. 309.
37. Zeng, Z., Natesan, K., and Maroni, V.A. *Oxidation of Metals*, vol. 58, 2002. pp. 147.
38. Chun, C.M., Ramanarayanan, T.A., and Mumford, J.D. *Materials and Corrosion*, vol. 50, 1999. pp. 634.
39. Chun, C.M., Mumford, J.D., and Ramanarayanan, T.A. *Journal of the Electrochemical Society*, vol. 147, 2000. pp. 3680.
40. Szakalos, P., Lundberg, M., and Petterson, R. *Corrosion Science*, vol. 48, 2006. pp. 1679.
41. Rosado, C. and Schütze, M. *Materials and Corrosion*, vol. 54, 2003. pp. 831.
42. Young, D.J., Motin, M.A.A., and Zhang, J. *Defects and Diffusion*, vol. 289–292, 2009. pp. 51.
43. Baker, B.A. and Smith, G.D. *Corrosion 2000*, NACE, Houston TX. Paper 257.
44. Nishiyama, Y., Moriguchi, K., Otsuka, N., and Kudo, T. *Materials and Corrosion*, vol. 56, 2005. pp. 806.
45. Toh, C.H., Munroe, P.R., Young, D.J., and Foger, K. *Materials at High Temperatures*, vol. 20, 2003. pp. 129.
46. Grabke, H.J. *Materials at High Tempereture*s, vol. 17, no. 4, 2000. pp. 483.
47. Grabke, H.J., Krajak, R., Müller-Lorenz, E.M., and Strauss, S. *Materials and Corrosion*, vol. 47, 1996. pp. 495.
48. Toh, C., Munroe, P.R., and Young, D.J. *Materials at High Temperatures*, vol. 20, 2003. pp. 527.
49. Ramanarayanan, T.A., Chun, C.M., and Mumford, J.D. US Patent 6,737,175.
50. Speck, P. and Young, D.J. US Patent 13/552,923. ◆